CHARGED PARTICLE ACTIVATION ANALYSIS OF LIGHT IMPURITY ELEMENTS IN SEMICONDUCTOR MATERIALS

T. Nozaki
RIKEN, Wako-shi, Saitama 351-01, Japan

Abstaract

By charged particle activation analysis C, N and O in semiconductor materials can be determined reliably usually down to 1 ppb. Using the classical RIKEN Cyclotron for this analysis, we elucidated the phase diagramme, IR absorptivity and behaviour of C, N and O in Si. We also analyze C and O in GaAs and O on surfaces and in epitaxial films.

1. Introduction

This year we have celebrated 50th aniversary of the invention of activation analysis by Hevesy and Levi.[1] They determined dysprosium in yttrium oxide using an isotopic neutron source. In Japan Sagane reported activation analysis of sodium in aluminium by the $^{23}Na(d,n)^{24}Na$ reaction in 1942.[2] He used the oldest cyclotron of RIKEN.

In 1960 I was a researcher of the Electrical Communication Laboratory, which was within a cycling distance from INS. The first cyclotron of INS then was fully used mainly for nuclear physics by research groups from various parts of Japan. One day I hit on an idea that by the use of a cyclotron we could determine sub ppm levels of impurity O and that the determination of O and C would soon become essential in semiconductor sciences. Professor Nonaka, the chief of INS, kindly offered us some cyclotron machine time, which was very, very precious at that time. We utilized this machine time for the analysis of O in Si by the $^{16}O(\alpha,pn)^{18}F$ reaction, and succeeded in demonstrating its usefulness.[3,4] A few years later I moved to RIKEN, where a variable-energy, classical-type cyclotron was under construction. Since 1967 we have used this cyclotron for activation analysis and radioisotope production.

What we have so far established, measured or obtained by this analysis can be summarized as follows: (1) methods for determining down to 1 ppb of O in almost all semiconductor materials and metals and 1 ppb of C and N in Si and C in GaAs;[5,6] (2) O, N and C concentrations in Si at various atages of its industrial production processes;[5] (3) phase diagrammes for extremely low concentration ranges of O, N and C in Si;[5,7] (4) calibration curves for IR spectrophotometry of O, N and C in Si;[5,8,9] (5) solubility and diffusion constant of O in solid Si at various temperatures by specially devised apparatus for activating O with an equal probability along the sample depth;[10,11] (6) decrease of O concentration in crystal formation of Si heavily doped with Sb;[12] (7) methods of analyzing C in different states in Si separately;[5] (8) methods for analyzing surface O under any atmospheric condition; (9) quantity and position of O in silicon nitride films using nuclear recoil;[13] and (10) concentration and behaviour of O in GaAs.[14] Also some metals were analyzed for O and C. Now the following studies are in progress: (1) utilization of ^{15}N as activable tracer in solid state sciences, with the activation by the $^{15}N(\alpha,n)^{18}F$ reaction; and (2) analysis of C in GaAs for the determination of IR calibration curve and for the elucidation of its effect on electronical properties.

In this article, (1) characteristics and procedure of charged particle activation analysis are given, (2) main part of our works are surveyed, and (3) present status and future prospect are shown of the activation analysis together with obstacles in our present situation.

2. Characteristics and Procedure

2-1. Characteristics

Of many methods of high-sensitivity analysis, charged particle activation analysis is the most reliable and sensitive for the determination of C, N and O, which are hardly activated by thermal neutron. These elements are abundant in nature, and the determination of their trace amounts in a sample bulk is likely to be interfered with contaminations on surface and from environment. In activation analysis, the surface contamination can be removed by etching after the activation and non-radioactive contamination after the activation need not be taken into account. In quantitative analysis of trace amounts of C, N and O, standard substances (comparators) of well-defined stoichiometry and good thermal stability, such as graphite, AlN and SiO_2, can be used more appropiately in charged particle activation analysis to give more accurate results than any other method. Hence, charged particle activation analysis is effective for the standardization of other methods. Also, charged particle activation analysis can be used for the analysis of surfaces and epitaxial films, under suitable selection of bombardment conditions.

In this method, however, there are restrictions in thermal and radiation stability as well as size and shape of the sample, which should usually be cooled during the bombardment. Also there are more interference reactions in this method than in neutron activation analysis. Further, experiences of higher levels are often required in charged particle activation analysis than many other methods.

2-2. Activation Reactions

Nuclear reactions useful for the activation of C, N and O are given in Table 1. The excitation function for the $^{16}O(^{3}He,p)^{18}F$ reaction is shown in Fig. 1, together with the activation probability of O and the range-energy relation of ^{3}He in Si. It is generally true that the sensitivity of analysis increases with the incident energy but the interference becomes much more serious with it. Especially the low-Z-fission of the matrix itself sometimes interferes most seriously. Fig. 2 shows the thick target yields of ^{11}C, ^{13}N and ^{18}F for ^{3}He and α-particle induced fission of the Si matrix itself.

2-3. Procedure

The experimental procedure consists of (1) sample preparation, (2) bombardment, (3) surface contamination removal, (4) chemical separation, (5) activity measurement, and (6) carrier-recovery measurement. Sometimes Steps 4 and 6 are not necessary. The sample is preferred to be a plate of 150 X 150 X 0.5 - 1 mm dimension with flat surfaces, though smaller pieces can also be analyzed. It is set on a water-cooled target holder, and bombarded in cyclotron vacuum or in

Table 1. Activation Reactions for C, N and O

Element	C	N	O
Activation Reaction	$^{12}C(^{3}He,\alpha)^{11}C$	$^{14}N(p,\alpha)^{11}C$	$^{16}O(^{3}He,p)^{18}F$
Interference Reactions	$^{9}Be(^{3}He,n)^{11}C$ [0] $^{10}B(^{3}He,d)^{11}C$ [0] $^{14}N(^{3}He,\alpha d)^{11}C$ [10.2] $^{16}O(^{3}He,2\alpha)^{11}C$ [6.3] $^{28}Si(^{3}He,^{20}Ne)^{11}C$ [11.3]	$^{11}B(p,n)^{11}C$ [3.1] $^{12}C(p,d)^{11}C$ [18.0]	$^{19}F(^{3}He,\alpha)^{18}F$ [0] $^{20}Ne(^{3}He,\alpha p)^{18}F$ [3.1] $^{23}Na(^{3}He,2\alpha)^{18}F$ [0.4] $^{27}Al(^{3}He,3\alpha)^{18}F$ [11.8] $^{30}Si(^{3}He,^{15}N)^{18}F$ [11.5]
Suitable Incident Energy	15 MeV	12 MeV	15 MeV
Other Useful Reaction	$^{12}C(d,n)^{13}N$		$^{16}O(p,\alpha)^{13}N$ $^{16}O(t,n)^{18}F$

The figures in square brackets indicate the threshold energy in MeV. for silicon matrix.
^{11}C, ^{18}F and ^{13}N are all pure positron emitters with half-lives of 20 m, 110 m and 10 m, respectively.

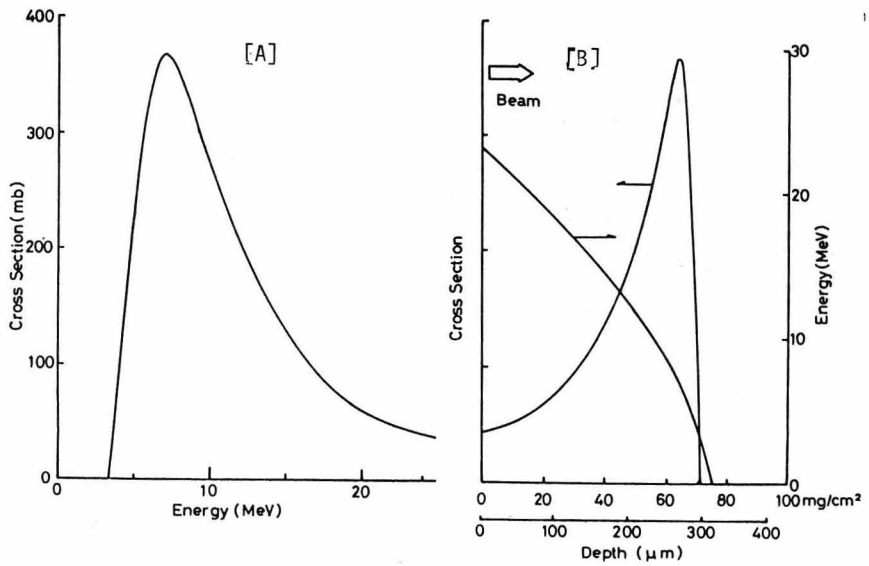

Fig. 1. (A) Excitation function for the $^{16}O(^{3}He,p)^{18}F$ reaction, and (B) ^{3}He energy and reaction cross section in relation with sample depth (sample: Si; incident ^{3}He energy: 23 MeV).

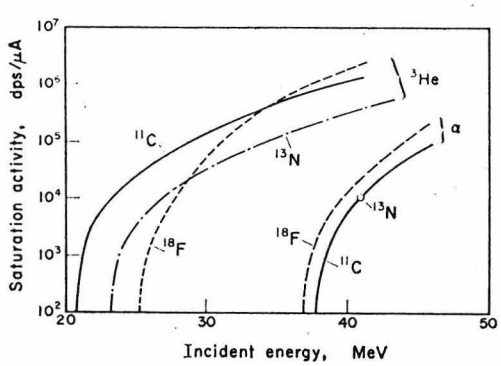

Fig. . Thick target yield of ^{11}C, ^{13}N and ^{18}F for ^{3}He and α-particle induced low-Z-fission of Si.

a helium stream. The beam should be of such a shape as to impinge entirely on the sample, and its intensity should be made as homogeneous as possible in its cross section. Total beam intensity should be determined from the thermal stability of the sample (usually 1 to 10 μA) and kept as constant as possible during each bomnardment. The bombardment duration is selected from the half-life of the nuclide to be measured and from machine-time economy. The beam current is integrated by a current integrator, under consideration on secondary electrons.

Experiences are necessary in the surface contamination removal. A surface layer about 5 mg/cm^2 thick should be removed uniformly. For chemical separation, details will be given later. The radioactivity after chemical separation is usually measured by a scintillation counter, but a germanium detector is often required for nondestructive measurement. Coincidence measurement of the annihilation radiation is often the most useful in the analysis of ppb level impurities, though its counting efficiency is more sensitive

to sample geometry than the efficiency of other detectors. A pair of BGO (bismuth germanium oxide) detectors with 2" X 2" size which we now use is of about 20 % efficiency with background counts of about 1.2 cpm.

The activation standard is covered with an aluminium foil of a thickness equivalent with the sample surface thickness removed by the etching, and bombarded with a lower beam current and for a shorter time. The difference of the energy-range relation between the sample and standard should be taken into account in the calculation of the final result.

3. C, N and O in Si

3-1. Semiconductor Silicon and Light Impurity Elements

It is now the age of semiconductor silicon. This substance is produced by the following processes: (1) reduction of quartz (SiO_2) with carbon (coke) to give crude elemental Si, (2) its conversion into $SiHCl_3$ or SiH_4, followed by purification of this compound by fractional distillation, (3) thermal decomposition of the purified substance to give polycrystals of high-purity elemental Si, and (4) single-crystal formation by Czochralski (CZ) or float zone (FZ) process. Metallic impurities and B had been studied fairly well already 20 years ago. As for C in Si, the analysis was undertaken since 1950s, and values between 10 and 100 ppm were reported in the former half of 1960s. In late 1960s, C contents of Si measured by charged particle activation analysis and IR spectrophotometry all are situated between 0.02 and 4 ppm. This great difference is due not to the elevation of the Si purity itself but to the fault in the older methods of analysis.

In Si, 1 wt ppm for C, N and O are equal to 1.17 X 10^{17}, 1.00 X 10^{17} and 0.88 X 10^{17} at./cm^3 and also to 2.3, 2.0 and 1.8 at ppm, respectively.

3-2. Determination of C, N and O in Si

Silicon itself gives radioactivities of only ^{30}P (β^+, 2.5 m) in the proton bombardment and ^{30}P and ^{31}Si (β^-, 2.6 h, weak γ-intensity) in the ^3He bombardment. Oxygen is almost always the predominant impurity in semiconductor Si. Thus an O concentration over 10 ppb in Si can be determined nondestructively by the $^{16}O(^3He,p)^{18}F$ reaction. For a concentration over 0.5 ppm, a germanium detector is also useful and often preferred. The reproducibility of this determination has been proved by repeated analysis of a silicon wafer with presumably homogeneous O concentration at different cyclotron machine times in 1982, 1983 and 1985, to give the following results: 10.20, 10.08, 10.12 and 10.23 ppm in 1982; 10.28 ppm in 1983; 9.86, 9.71, 10.05 and 9.87 ppm in 1985; mean, 10.10 ± 0.18 ppm.

For very low O concentration in Si, chemical separarion is needed. The bombarded silicon after the surface contamination removal by etching with $HF-HNO_3$ is pulverized and dissolved in a KOH solution containing KF (2 g) as carrier. The F is precipitated first as LiF, which is collected by filtration and then converted into KBF_4 precipitate by treatment with HCl containing H_3BO_3 and KCl. The counting form is this KBF_4, and the carrier recovery is measured simply by weighing. This method is sensitive down to 300 ppt of O, though the lowest concentration of O ever found has been about 2 ppb.

Chemical separation of ^{11}C is almost always necessary in the analysis of C and N in Si by activation with the $^{12}C(^3He,\alpha)^{11}C$ and $^{14}N(p,\alpha)^{11}C$ reactions. The bombarded sample after the surface etching and pulverization is dissolved in a NaOH solution containing Na_2CO_3 (2 g) as carrier in a quartz vessel, and $KMnO_4$ (2 g) is added to it. The solution is then heated in a microwave oven, until it becomes a melt with dark red brightness (700 - 800 °C). After cooling, the content of the vessel is treated with H_2SO_4 to generate $^{11}CO_2$, which is caught by a methanolic solution of LiOH to give Li_2CO_3 precipitate. This is the counting form. The carrier reconvery is measured by weighing. The reliability of this separation was checked by the use of Si conatining only ^{11}C as β^+ emitter. This was prepared by proton bombardment of B-doped Si, and the ^{11}C formed by the $^{11}B(p,n)^{11}C$ reaction in Si was measured before and after the chemical separation. The sensitivity of this method is 1 ppb for C and N.

3-3. C, N and O Contents of Semiconductor Si [5]

The results of C and O analysis for various commercial semiconductor Si are shown in Table 2. These are for rather old products; at present C content has decreased to half or further less, though O content has remained almost the same. Table 3 gives the change of C and O contents of Si in industrial production. The C and O contents are shown to depend on the conditions in single-crystal formation rather than the method of chemical purification. Nitrogen content was found always less than a few ppb.

Table 2. C and O content of commercial semiconductor Si

	C content 10^{17} at./cm^3	O content 10^{17} at./cm^3
Polycrystal	0.20 - 0.50 [0.82]*	0.80 - 3.0 [0.40]*
Single crystal		
FZ in argon	0.080 - 0.35	0.05 - 0.20
FZ in vacuum	0.030 - 0.40	0.010 - 0.030
CZ in argon	0.30 - 3.0	2.0 - 10
Dislocation-free FZ	0.40, 0.13, 0.016, 0.30	0.013, 0.019, 0.026, 0.10

* Figures in the brackets are exceptional values.

Table 3. Change of C content in an industrial process

	C content 10^{17} at./cm^3	O content 10^{17} at./cm^3
Crude	40	10
Polycrystal	0.20 - 0.50	0.80 - 0.85
FZ in argon*		
(Single pass)	0.15	0.06
FZ in vacuum*		
Single pass	0.03	0.03
Three passes	0.02	0.015
CZ in argon	1.0	4

* Middle portion of the rod.

3-4. Phase Diagrammes for Extremely Low Concentrations of C, N and O in Si [5,7]

From the logarithmic form of the entropy of mixing, it is clear that any two substances are missible, no matter sometimes how small the solubility may be. There should thus exist eutectic or peritectic points in the phase diagrammes of C-Si, N-Si and O-Si systems at extremely low concentration ranges of C, N and O. These phase diagrammes were unknown before our study. Here is shown the experimental procedure by which we elucidated the phase diagramme for C-Si system.

Various quantities of C (10, 30 and 100 ppm) in aqueous suspension (trade name, Aquadag) were painted uniformly on silicon rods (2.5 cm diameter, 30 cm length), and a molted zone was passed through them in vacuum. In this process, SiC particulates appeared on the surface of the melt; the larger the quantity of C painted, the sooner the appearance of the particulates. The rods were then sliced and C in each slice was determined by charged particle activation analysis. The resultant C distribution in one of the rods is shown in Fig. 3. Carbon concentration just before the appearance of SiC was found always (3.5 ± 0.4) X 10^{17} at./cm^3 regardless of the quantity of C painted on the rod. This is explained clearly by the phase rule;

when three condensed phases (e.g., solid Si, liquid Si and SiC) and a gas phase coexist in equilibrium in a two-compoment system (e.g., C and Si), the composition of each phase should be determined uniquely. Hence, $(3.5 \pm 0.5) \times 10^{17}$ at./cm^3 is the solubility of C in Si at its melting point.

Next, molten zones were passed with various travelling velocities in several parts of one of the rods, where there was no SiC particulates. The resultant C distribution was then measured by slicing and charged particle activation analysis. The results are shown in Fig. 4. From this the effective distribution coefficient of C in Si is obtained in relation with zone

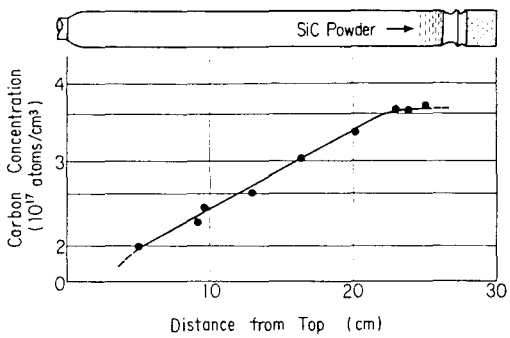

Fig. 3. Carbon distribution after a single zone pass through a carbon-painted silicon rod.

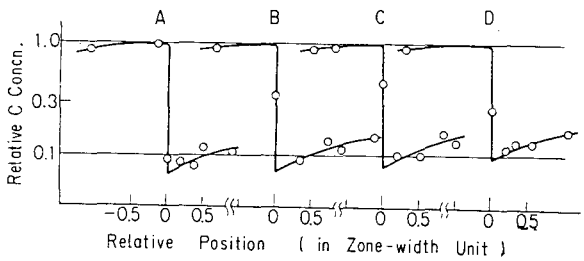

Fig. 4. Carbon distribution for various zone velocities. Zone travelling velocity: A, 0.4 mm/min; B, 0.8 mm/min; C, 1.2 mm/min; D, 1.6 mm/min.

velocity as shown in Fig. 5. By extrapolating the curve in Fig. 5 to zero velocity, we can obtain the equilibrium distribution coefficient of C in Si as 0.07 ± 0.01. Based on the two constants thus obtained, we can draw the phase diagramme of C-Si system at extremely low C concentration range, as in Fig. 6.

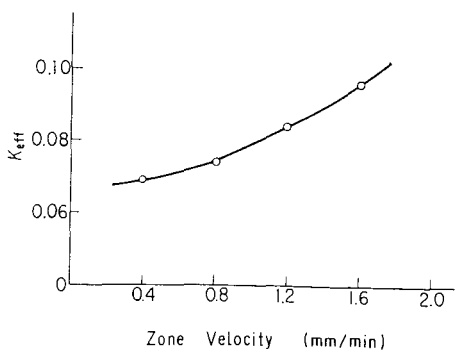

Fig. 5. Effective distribution coefficient of C in Si vs. solidification rate.

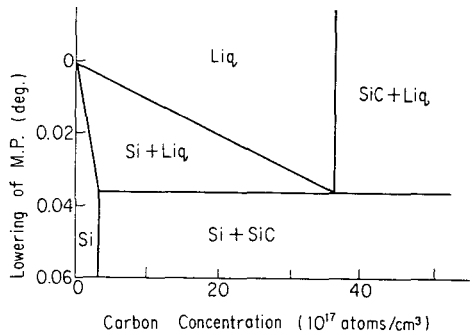

Fig. 6. Phase diagramme of C-Si system in extremely low C concentrations.

Although there were some difficulties due to the volatility of N and O, we obtained the phase diagramme for N-Si and O-Si systems by analyzing samples prepared by zone-melting and sudden solidification under selected conditions. They are given in Figs. 7 and 8. The numerical value of these results are given in Table 4. Much attention has been paid to C, N and O impurities in science and technology of semiconductor Si, and these data are now shown in various data books.[15]

3-5. Calibration Curve for IR Spectrophotometry [5,8,9]

Although inferior to charged particle activation analysis in sensitivity, IR spectrophotometry can also be used for C, N and O in Si and is actually used for routine analysis. Semiconductor Si is now an international trade commodity and the control of its C and

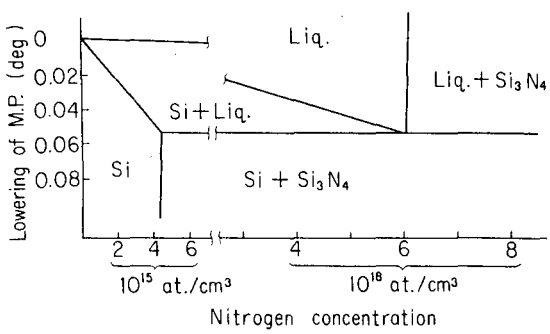

Fig. 7. Phase diagramme for N-Si system in extremely low N concentrations.

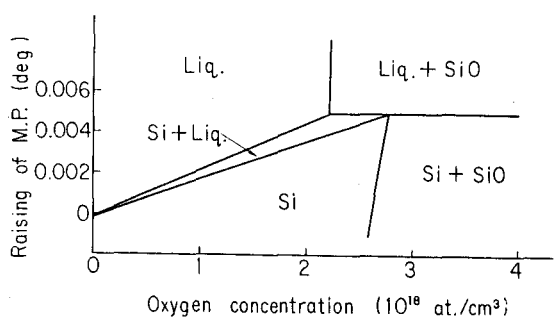

Fig. 8. Phase diagramme for O-Si system in extremely low O concentrations.

Table 4. Solubilities of C, N and O in Si at its melting point and their equilibrium distribution coefficient.

Impurity	Solubility in solid Si		Solubility in liquid Si		Equilibrium distribution coefficient
	10^{17} at./cm^3	ppm at	10^{17} at./cm^3	ppm at	
C	3.2 ± 0.3	6.5 ± 0.5	45 ± 5	90 ± 10	0.07 ± 0.01
N	0.045 ± 0.010	0.09 ± 0.02	60	120	7×10^{-4}
O	27.5 ± 1.5	56 ± 3	22.0 ± 1.5	45 ± 3	1.25 ± 0.17

O contents is needed. It has thus become indispensable to get highly reliable calibration curves for them and to use the curves all over the world. The calibration curves reported before, however, were noticeably different from one another. In Japan a committe was organized for getting satisfactory calibration curves and also for preparing silicon wafers of various, accurately known O and C concentrations to distribute widely as IR standards.

Silicon wafers of 2, 1 and 0.5 mm thick with various O concentrations, 70 wafers in all, were prepared and submitted to round robin IR measurement by about 20 laboratories including foreign laboratories. The 1 mm wafers, 22 in all, were then analyzed by charged particle activation. The analysis of each wafer was repeated at least twice. Samples for which the results of the two analyses deviated more than 5 % were analyzed once again. When the three analyses gave no satisfactory results, the fourth analysis was undertaken. Within each cyclotron machine time usually 8 silica plates were bombarded as the activation standard in order to elevate the reliability.

Fig. 9 shows the resultant calibration curve, which agrees completely with our previous curve.[5] We believe that this result is by far the most reliable. National Bureau of Standard, U.S.A., however, wanted to repeat similar procedure in world-wide scale. In Japan we already finished the measurement; the results are practically the same as before.

The calibration curve for substitutional C in Si has been obtained; it is shown in Fig. 10. Since the destructive chemical separation was necessary in activation analysis, wafers in adjacent positions in the crystal were analyzed to ascertain the reproducibility. The results of activation analysis were corrected for (1) the difference in counting effciency of ^{11}C between the graphite activation standard and the separated Li_2CO_3 and (2) the interference of the $^{16}O(^3He,2\alpha)^{11}C$ reaction, after careful examination of the two correction values. In Fig. 9 are also given results of secondary ion mass spectrometry (SIMS). The SIMS workers draw a strait line paralell to the activation analysis line, regarding the difference between the two lines as the background in SIMS.

Apart from the committee work, we obtained the calibration curve for N in Si.[9] For as-grown FZ silicon, it is expressed as

[N concentration (at./cm^3)] = (1.83 ± 0.24) X 10^{17} [Absorption coefficient (963 cm^{-1} peak, room temperature)].

Since the solubility of N in Si is very low, various difficulties existed in both IR measurement and accurate activation analysis. The absorptivity of N was found to be less than the above value for CZ Si and heat-treated FZ Si, indicating the presence of IR-insensitive N in these Si.

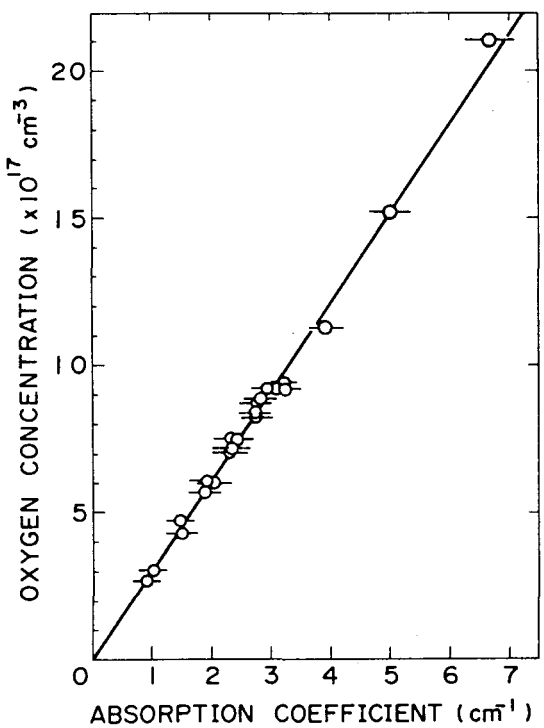

Fig. 9. Calibration curve for IR spectrophotometry of O in Si. For 1100 cm^{-1} absorption peak, at room temperature.

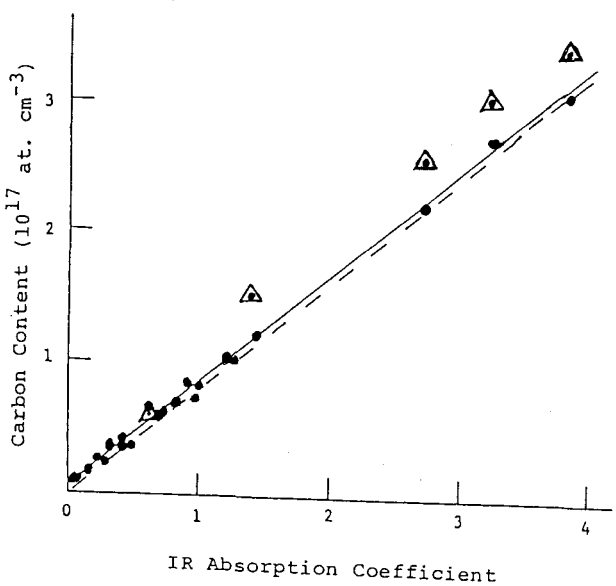

Fig. 10. Calibration curve for IR spectrophotometry of C in Si (605 cm^{-1}, room temperature).
Solid line: before the correction for C in IR reference Si (C concentration: 4.3 X 10^{15} at./cm^3).
Dotted line: after the correction.
△ : results of SIMS.

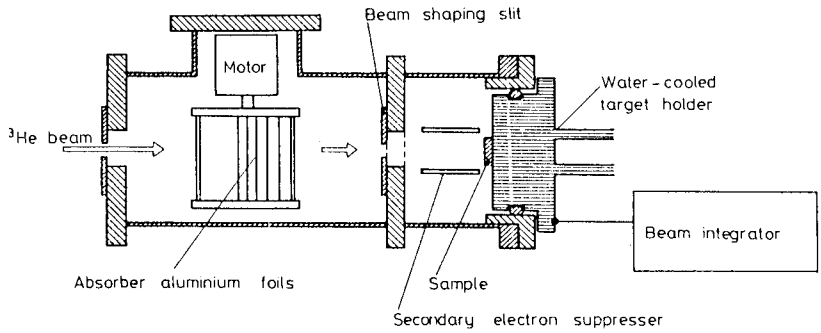

Fig. 11. Apparatus for activation of O with equal probability along depth.

3-6. Solubility and Diffusion Constant of O in Si ---- -- Use of Activation with Equal Probability along Depth [10,11]

In charged particle activation, an impurity homogeneously distributed in a sample gives radionuclide depth profile determined by the excitation function and range-energy relation. This is exemplified in Fig. 1 by the ^{3}He activation of O in Si. By properly selected periodic change of the incident particle energy, the impurity can be activated with equal probability up to a certain depth of the sample. Such an energy change can be realized by the rotation of a set of aluminium foils with selected thicknesses and widths across the incident particle beam. Using 8 sheets of foil, we substantiated an activation curve which was constant within 5 % up to about 250 μm depth in Si. The incident ^{3}He energy was set at 22 MeV, above which Si itself gives ^{18}F by low-Z-fission. The apparatus is shown in Fig. 11.

Using this activation followed by step-etching, we can obtain the depth profile of O. Silicon wafers of various O contents were heated in O_2 at given temperatures, and the resultant O depth profiles were measured; the results for 1100 °C are shown in Fig. 12. The extrapolation of each curve in Fig. 12 to the sample surface gives the same O concentration, regardless of the initial O content of the sample. It is clear that this concentration is the solubility of O in solid Si at this temperature. From the curves in Fig. 12, we can also obtain the diffusion constant of O. Since the experiment was carried out for other temperatures, the solubility (S) and diffusion constant (D) were obtained as follows:

$$S = 9.3 \times 10^{21} \exp[-27.6 \text{ kcal mol}^{-1}/RT] \text{ at./cm}^3$$
$$D = 3.2 \exp[-67.1 \text{ kacl mol}^{-1}/RT] \text{ cm}^2/\text{s}.$$

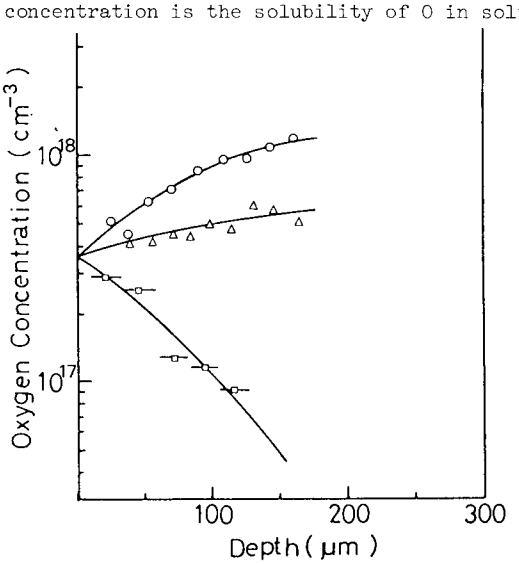

Fig. 12. Oxygen profiles in Si heat-treated in O_2. Heat treatment: 1100 °C, 114 h. Initial O content of Si: ○ , 10 X 10^{17}; △ , 6 X 10^{17}; □ , 0.05 X 10^{17} at./cm^3.

4. O and C in GaAs

4-1. Method of Analysis

The analysis of GaAs for O and C is rather difficult, because of the low thermal stability and low O and C contents as well as high radioactivities formed from itself. We made a lot of efforts for separating ^{18}F from bombarded GaAs, and finally established the following very satisfactory procedure in which properties of KBF_4 are utilized: (1) dissolution of the sample in HCl-HNO_3 containing F^- carrier (2 g), (2) addition of H_3BO_3 and K^+ to the solution to precipitate KBF_4, (3) dissolution of collected KBF_4 in hot dil HNO_3, (4) successive addition of HBr (100 mg) and $AgNO_3$ (300 mg) to the hot solution, and the removal of AgBr precipitate, (5) addition of K_3BO_3 to the solution and its cooling to precipitate KBF_4, and (6) collection of the precipitate for counting. The carrier recovery is measured by weighing. By this method down to 1 ppb of O in GaAs can be measured. With slight modification or often with simplification, this ^{18}F separation can be applied successfully to almost all matrices; one example is already shown in Sect. 3-2.[6]

The ^{12}C(d,n)^{13}N reaction is used for the activation of C in GaAs, because of the interference of B in the ^{3}He activation (see Table 1). Usually GaAs contains much more of B than C. For quick separation of the ^{13}N, dry fusion is useful. The bombarded sample is fused with Cu by RF heating in a helium stream. The ^{13}N is volatilized completely within 5 min, and is carried with the helium stream through successive columns of Cu powder at 900 °C, CuO at 900 °C, Ascarite (NaOH) at room temperature, and titanium sponge at 900 °C in which it is caught as titanium nitride. In this method, quantitative separation is essential because of the difficulty of carrier-recovery measurement; it is chequed by the use of ^{13}N-implanted GaAs prepared by proton bombardment of O_2 in a narrow gap between two GaAs plates. A part of ^{13}N formed by the ^{16}O(p,α)^{13}N reaction was implanted into the GaAs by nuclear recoil. The sensitivity for C in GaAs is now about 1 ppb. In this process B can also be determined simultaneously by the measurement of ^{11}C formed by the ^{10}B(d,n)^{11}C reaction and trapped in the Ascarie column.

4-2. Results

The contents of O and C of present commercial GaAs are very low as compared with Si, Ge and many high-purity metals, being mostly less than 50 ppb for both. It was found that the dopind of O is difficult owing

probably to the volatility of As_2O_3 and that apparent distribution coefficient of O between solid and liquid GaAs was about 2 in HBG (holizontzl boat grown) process.[14]

Similarly as O and C in Si, the committee is now working to obtain reliable calibration curve for IR spectrophotometry of C in GaAs. Our preliminary results indicate that the calibration curve ever obtained from electrical conductivity gives apparent C contents higher by a factor of 2 or 3 than the true values. Various other studies are now in progress concerning C in GaAs, and interesting results can be expected.

5. Analysis of Surfaces and Films on Plates [13]

Oxygen on surfaces and in films on plates is also analyzed quantitatively and reliably by activation with the $^{16}O(^3He,p)^{18}F$ reaction. There are following sources of contamination in cyclotron bombardment: (1) ^{18}F formed from residual O in the bombardment vessel, and (2) ^{18}F formed on the backside surface of the beam-entrance window and recoiled onto the sample. In our experiment, thus, two identical sample plates were kept in good contact with their surfaces to be analyzed inside, and bombarded under evacuation with oil-free pumps. Fig. 13 shows the arrangement of sample in the analysis of silicon nitride epitaxial films.[13] Incident ^3He energy is so selected as to give nearly the maximum cross section at the surfaces or films to be analyzed. After the bombardment the surfaces or films are removed from the sample bulk chemically or mechanically, and their ^{18}F activity is measured. Often only the forward sample is required for the measurement, because of the nuclear recoil of ^{18}F. In general, from 5 to 300 ng/cm^2 of O is found on any surface just after etching. It is easily shown by calculation that O on the surface is much more than O in air between two flat plates in good contact even under 1 atm.

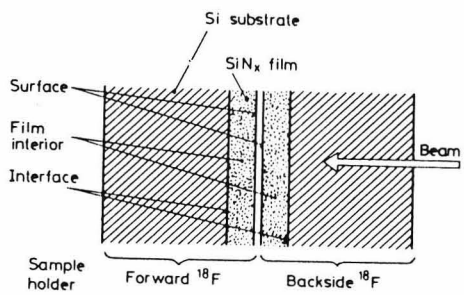

Fig. 13. Sample arrangement and O locations in film.

In the analysis of films, not only the total O is determined but also the location of its predominant part is estimated to be whether on film surface, in film interior, or on film-substrate interface (Fig. 13). For this, however, samples with varying thicknesses but otherwise identical are required, and the ^{18}F in the backside sample and in the forward sample (Fig. 13) should be measured separately. The sum of the two ^{18}F quantities gives the total O. When the sum is plotted against the thickness, the slope of the resultant curve gives O concentration in the film and the intercept of ordinate is the sum of O on film surface and on film-substrate interface. Because of the nuclear recoil, the fraction of ^{18}F found in the backside sample (1) remains always almost zero for O on film surface, (2) increases slightly with film thickness for O in the film, or (3) increases pronouncedly for O on film-substrate interface. The results are shown in Table 5 for plasma-epitaxy silicon nitride films on silicon wafers prepared under two slightly different conditions. As for quantitative forward recoil range, we measured its distribution for various ^{18}F-formation reactions.[16]

6. Present Status and Future Prospect

There are now a lot of needs for charged particle activation analysis of C, N and O from semiconductor companies and from some organizations which intend to make fine use of metals. These needs will clearly increase in future, and continuous efforts should be made for normalization and automation of the analytical procedure in order to increase the efficiency and minimize worker's labour and radiation exposure. Our techniques now can meet present needs. For various compound semiconductors, however, some improvement will soon become necessary in sensitivity and accuracy of the analysis, because C, N and O are often electronically active impurities in them. For O, triton activation with the $^{16}O(t,n)^{18}F$ reaction gives much higher sensitivity with much less interference than the ^3He activation.[17] In foreign countries, too, charged particle activation analysis has mostly been studied and used for similar purposes as ours.

Sometimes charged particle activation analysis is used for nondestructive, multi-element analysis, just like thermal neutron activation analysis. The use of heavy-ion induced reactions, e.g., the $^1H(^{14}N,\alpha)^{11}C$ reaction for the determination of H, has been reported. In this analysis, however, the removal of surface contamination is very difficult, because the product nuclide is recoiled into almost the same depth regardless of the position of its formation.

Facilities for charged particle activation analysis is now quite limited. In Japan only three cyclotrons are available for it. In order to make this method more beneficial widely for public, Japan Chemical Analysis Center now undertakes trust analysis on semi-commercial bases using RIKEN Cyclotron and techniques we developed. The elements and matrices acceptable by this trust analysis is shown in Table 6, together with the lowest guaranteed level of determination. We are making efforts to increase the variety of matrices analyzable in this trust analysis.

Table 5. Quantity and location of O in silicon nitride epitaxial films on Si wafer.

Sample type	Oxygen quantity		Film-thickness dependence of back-side ^{18}F fraction	Main oxygen location
	Total quantity	Film-thickness dependence		
A	Large (0.4 - 2 μg/cm^2)	Linear increase with thickness	Slight increase with thickness	Film interior (0.2 - 0.6 wt%)
				Surface (0.4 - 1.0 μg/cm^2)
B	Small (0.2 - 0.3 μg/cm^2)	Independent of thickness	Pronounced increase with thickness	Interface (0.2 - 0.3 μg/cm^2)

Table 6. Elements and matrices analyzable by our trust analysis

Matrix	Element	Guaranteed lowest level (ppb wt)
Si	C	20
Si	N	10
Si	O	5
GaAs	O	5
Al	C	5
Al	O	10
AlN	O	*
BN	O	*

* Depending on coexisting elements, but always enough sensitivity.

7. Requirements to Cyclotron Engineers and Ploblems in Our Present Situation

As can be understood from Table 1 and Sect. 2-3, requirements to cyclotron engineers from workers of routine activation analysis are rather simple. Beam homogeneity within its cross section, ease in operation and beam shaping, and stability are essential for popular use of cyclotrons for this purpose. For fundamental research related to the method and technique themselves of activation analysis, an accelerator with slightly higher energy (e.g., 25 MeV p, 30 MeV ^{3}He) is preferred. With a suitable safe handling system, a triton cyclotron of 10 MeV energy will surely be of high value for the analysis of ultra-trace O.

In RIKEN now the SSC is under construction, and this needs an enormous expenses. Funds for studies by the use of other accelerators have thus been badly suppressed in these few years, as is often the case. For every accelerator-based study, there exists an incident energy range essential or most often useful. Since RIKEN consists of nearly 50 laboratories covering vast fields of science and technology, we are urged to hit on new ideas of accelerator utilization in multidiciplinary fields. Hence, various accelerators are needed in RIKEN. Good works in an application field are almost always guided by wide-viewed new idea combined with high-level experiences in this field. I, as an user of accelerator in chemistry, would like to say frankly that we should strive to undertake researches that are originality- or idea-initiated rather than machine-led.

Acknowledgements

The author should like to express his thanks to (1) permanent and temporary members and visiting staffs of RIKEN Radiochemistry Laboratory, (2) RIKEN Cyclotron Operating Group, and (3) various semiconductor companies in Japan, for their collaborations and helps.

References

1. G. Hevesy and H. Levi, Mathematisk-Fysiske Meddelelser., 14, 3 (1936).
2. R. Sagane, M. Eguchi and J. Shigeta, Proc. Physico-mathem. Soc. Japan, 16, 383 (1942).
3. T. Nozaki, S. Tanaka, M. Furukawa, and K. Saito, Nature, 190, 39 (1961).
4. K. Saito, T. Nozaki, S. Tanaka, M. Furukawa, and H. Cheng, Int. J. appl. Radiat. Isotopes, 14, 357 (1963).
5. T. Nozaki, Y. Yatsurugi, N. Akiyama, Y. Endo, and Y. Makide, J. Radioanal. Chem., 19, 109 (1974).
6. T. Nozaki, J. Radioanal. Chem., 70, 329 (1982).
7. Y. Yatsurugi, N. Akiyama, Y. Endo, and T. Nozaki, J. Electrochem. Soc., 120, 975 (1973).
8. T. Iizuka, S. Takasu, M. Tajima, A. Arai, T. Nozaki, N. Inoue, and M. Watanabe, J. Electrochem. Soc., 132, 1707 (1985)
9. Y. Itoh, T. Nozaki, T. Masui, and T. Abe, Appl. Phys. Lett., 47, 488 (1985).
10. Y. Itoh and T. Nozaki, J. Radioanal. Chem., 70, 329 (1982).
11. Y. Itoh and T. Nozaki, Japan J. Appl. Phys., 24, 279 (1985).
12. T. Nozaki, Y. Itoh, T. Masui, and T. Abe, J. Appl. Phys., 59, 2562 (1986).
13. T. Nozaki, M. Iwamoto, K. Usami, and A. Hiraiwa, J. Radioanal. Chem., 52, 499 (1979).
14. H. Emori, M. Umehara, M. Takeya, K. Nomura, Y. Terai, and T. Nozaki, "Gallium Arsenide and Related Compounds 1981", Inst. Phys. Bristol, p. 47 (1982).
15. E.g., Landolt-Börnstein, "Zahlenwerte und Funktionen aus Naturwissenschaften und Technik", Neue Serie III/17c , Springer, Berlin, 1984, p.p. 33, 419, 420, 432, 434, etc.
16. M. Iwamoto, T. Nozaki, Y. Takahashi, and K. Usami, Radiochim. Acta, 30, 73 (1982).
17. T. Nozaki, M. Iwamoto and T. Ido, Int. J. appl. Radiat. Isotopes, 25, 393 (1974).